Published in final edited form as:
IEEE Trans Biomed Eng. 2014 February ; 61(2): 513–521. doi:10.1109/TBME.2013.2283369.

Biopsy using a Magnetic Capsule Endoscope Carrying, Releasing, and Retrieving Untethered Microgrippers

Sehyuk Yim [Student Member, IEEE],
Department of Mechanical Engineering, Carnegie Mellon University, Pittsburgh, PA 15213 USA

Evin Gultepe,
Department of Chemical and Biomolecular Engineering, Johns Hopkins University, Baltimore, MD USA

David H. Gracias [Member, IEEE], and
Department of Chemical and Biomolecular Engineering, Johns Hopkins University, Baltimore, MD USA

Metin Sitti [Senior Member, IEEE]
Department of Mechanical Engineering, Robotics Institute, and Biomedical Engineering, Pittsburgh, PA 15213 USA

Sehyuk Yim: samy@cmu.edu; Evin Gultepe: evingultepe@gmail.com; David H. Gracias: dgracias@jhu.edu; Metin Sitti: sitti@cmu.edu

Abstract

This paper proposes a new wireless biopsy method where a magnetically actuated untethered soft capsule endoscope carries and releases a large number of thermo-sensitive, untethered microgrippers (μ-grippers) at a desired location inside the stomach and retrieves them after they self-fold and grab tissue samples. We describe the working principles and analytical models for the μ-gripper release and retrieval mechanisms, and evaluate the proposed biopsy method in *ex vivo* experiments. This hierarchical approach combining the advanced navigation skills of centimeter-scaled untethered magnetic capsule endoscopes with highly parallel, autonomous, submillimeter scale tissue sampling μ-grippers offers a multifunctional strategy for gastrointestinal capsule biopsy.

Index Terms

Biopsy; capsule endoscopy; medical robotics; microgrippers (μ-grippers); minimally invasive surgery

Correspondence to: Metin Sitti, sitti@cmu.edu.

Color versions of one or more of the figures in this paper are available online at http://ieeexplore.ieee.org.

I. Introduction

Capsule endoscopy is a promising medical technology for minimally invasive diagnostics and therapeutics in the gastrointestinal tract [1]–[3]. However, currently, the clinical application of wireless capsule endoscopy is limited primarily to passive monitoring of the gastrointestinal tract via optical imaging modalities because clinicians have no control over the position and orientation of the capsules. Consequently, strategies are being pursued in the development of magnetically guided and actuated capsule robots for the next generation of capsule endoscopy. For example, Carpi *et al.* conducted animal experiments using a commercial magnetic actuation system (Niobe, Stereotaxis, Inc.), which was used for magnetic navigation of a cardiovascular catheter [4]. Hong *et al.* demonstrated feasibility of a magnetically actuated capsule in a pig's esophagus, stomach, and large intestine using a multi-degree-of-freedom robotic manipulator [5]. Swain *et al.* and Keller *et al.* conducted *in vivo* experiments using a manually manipulated external permanent magnet and multiple coils, respectively, [6], [7]. Abbot *et al.* investigated various magnetic manipulation methods and an electromagnetic device for capsule endoscopy [8], [9]. These experiments have demonstrated that magnetic manipulation is a useful modality for remote guidance of untethered capsule endoscopes.

Concurrently, an important challenge of active capsule endoscopes is the integration of on-board advanced diagnostic functions such as biopsy. To this end, various biopsy mechanisms for capsule endoscopes have been proposed. Kong *et al.* proposed a rotational biopsy device that was used to scratch the epithelial tissue in the small intestine of a rabbit [10]. Park *et al*. developed a spring-driven biopsy microdevice with barbed microspikes [11]. Simi *et al.* modified the design of Crosby–Kugler biopsy capsule [12] by applying a magnetic torsion spring mechanism to efficiently actuate a rotational razor in a small space [13]. These biopsy modules have shown feasibility in *ex vivo* experiments but have three main limitations for clinical applications. First, they are not capable of approaching a targeted tissue. Next, the actual workspace of the biopsy tools (e.g., rotational razor or microspikes) is out of sight of the on-board camera. Thus, it is not possible to observe tissue targeting and extraction. Finally, because they are activated only once, the success rate of reliable biopsy is significantly limited for each operation. These three issues are also highlighted in [14] where Kong *et al.* proposed a robotic biopsy device with multiple functional modules.

In this paper, we combine two multiscale robotic devices to implement biopsy in magnetic capsule endoscopy. The first robotic device is a centimeter-scaled untethered capsule, which is called magnetically actuated soft capsule endoscope [MASCE, Fig. 1(a)]. MASCE has one extra axial degree-of-freedom, which can be utilized for advanced functions such as controlled locomotion [15], localized drug delivery [16], gastric implant [17], 3-D localization and mapping of local tissue surface [18], and elastography [18]. The second one is a submillimeter scale self-folding microgripper [μ-gripper, Fig. 1(b)]. Previously, the μ-grippers were successfully utilized in *in vivo* endoscopic biopsy of hard to reach regions such as the bile duct inside live pigs [19]. The μ-grippers can be mass produced and respond to environmental cues such as temperature, and hence, they can operate autonomously in a highly parallel manner.

Our proposed multilength scale robotic approach combines the strength of autonomous and highly parallel biopsy using the μ-grippers with remote magnetic actuation, advanced therapeutic function, safe operation, and local targeting capabilities of the MASCE. We describe the working principles and analytical models for the μ-gripper release and retrieval mechanisms, and we evaluate the proposed biopsy method in *ex vivo* experiments.

We organized this paper as follows. In Section II, we introduce the MASCE-based biopsy scenario. In Section III, we introduce the capsule cargo, namely the μ-grippers. In Section IV, V, and VI, we focus on the locomotion, delivery, and retrieval methods of the MASCE, respectively, and describe their working principles. We present the *ex vivo* biopsy results in Section VII. In Section VIII, we discuss the impact and limitations of this study and the possibilities for future studies, and we conclude in Section IX.

II. Capsule Endoscope-Based Biopsy Strategy

The MASCE design with biopsy function includes three main units: locomotion, delivery, and retrieval [see Fig 2(a)]. To control its movement and direct the MASCE toward a specific location, we can utilize its locomotion unit, which can be controlled by an external magnetic field, as shown previously [15]. The delivery unit consists of a chamber for the cargo, in this case the μ-grippers, and is designed to be activated by a change in the strength of the applied magnetic field. When the applied magnetic field exceeds a predetermined value, the MASCE collapses and opens up the chamber to distribute its cargo. The retrieval unit, on the other hand, relies on wet-adhesive forces to trap the μ-grippers. It consists of silicone oil-coated micropost arrays placed at the tip of the capsule. It is also possible to add extra units such as a camera module to the MASCE without affecting its function. More detailed specifications of the biopsy-MASCE prototype are shown in Table I.

Fig. 2(b)–(d) summarizes the biopsy strategy using the μ-gripper-loaded MASCE. First, utilizing the magnetically actuated rolling locomotion of the MASCE, it is directed to the vicinity of the targeted region. When the MASCE is in close proximity to the target, the delivery unit is activated to distribute the μ-grippers on and around the target region. Next, the μ-grippers self-fold to their closed state after a predetermined time (10 min) after they are exposed to the body temperature. During self-folding, they grip and collect tissue samples from their surroundings. We, then, collect the closed μ-grippers together with the tissue samples using the retrieval unit of the MASCE.

III. Thermally Actuated Self-Folding Microgrippers

Taking inspiration from the multijointed design of human fingers, the μ-grippers were designed with flexible hinges interconnected with rigid phalanges [20]. The tip-to-tip size of the μ-grippers is 980 μm when they are open. When the hinges flex, the μ-grippers self-fold to their closed state. The energy required for the folding action is derived from the release of residual stress in the metallic bilayer hinges.

To control self-folding, we built the μ-grippers with a trigger mechanism, so that it can be actuated autonomously at the body temperature [19]. A thermo-sensitive polymer layer (mixture of (5:1 v/v) SC1805 and SC1813 MicroChem Corp., Newton, MA, USA) keeps the

prestressed hinges flat when they are at the room temperature. When the temperature is raised to the human body temperature (37 °C), due to the change in its modulus, the polymer layer cannot keep the hinges flat any longer and as a result the hinges flex and the μ-grippers close [see Fig. 3(a) and (b)]. Fig. 3(c)–(f) shows snapshots of μ-grippers closing at 37 °C. The details of the fabrication protocol of μ-grippers can be found in [21].

We optimized the μ-grippers so that they fully close 10 min after they are exposed to the body temperature. This prevents the premature closing of μ-grippers before their release using gastrointestinal capsule endoscopy. If needed, it is also possible to change the closing duration of the μ-grippers by adjusting the type and dimensions of the polymer trigger and underlying bilayer.

The μ-grippers were previously utilized to introduce the concept of stochastic biopsy strategy to screen large-area organs [22]. The conventional definition of the term biopsy comprises one-task-by-one-tool action where the operators extract tissue samples from a precisely targeted area. In contrast, in stochastic biopsy, a multitude of randomly distributed tools (such as the μ-grippers) collect tissue samples simultaneously. The stochastic biopsy method relies on the self-folding action of the μ-grippers; while they are closing, they grab and collect samples from the tissue around them. Also, since they respond to an environmental cue, temperature, they can be actuated in a highly parallel manner in large numbers; resulting in the collection of multiple tissue samples [22].

IV. Target Detection via On-Board Camera During Magnetically Controlled Locomotion

For a successful biopsy, it is necessary for the capsule endoscope to accomplish two main tasks. First, the capsule endoscope should be able to reach the target site. Second, targets need to be observed via an on-board camera. Previously, we introduced the rolling locomotion strategy of the MASCE using external magnetic fields in a gastric phantom [15]. The proposed magnetic actuation method is useful to control the motion of the capsule robot because the orientations of the capsule robot and the external magnet are symmetrical to each other. In this paper, we also evaluated whether the capsule robot can detect targets during the locomotion via an on-board camera.

We conducted *ex vivo* experiments using a fresh pig stomach and the MASCE prototype that has an on-board camera (CCIQ-II, *Misumi Electronics*, Taiwan). Because a wireless communication circuit and batteries were not integrated in the capsule prototype, yet we provided the power to the camera module and obtained the video output signals using thin wires. In the experimental procedure, first, we placed a fresh pig stomach on a maneuvering post and wet the tissue surface with saline. We did not fill the stomach with water because the image quality of our current camera module without an optical dome becomes poor in liquid, which will be improved in the future. We, then, dropped the MASCE prototype on the tissue surface, guided it to two targeted positions in succession and returned it back to the start point. Because the wires could induce an undesired tension during the rolling locomotion experiments, we fixed them on the maneuvering post using a tape, which

lessened the tension significantly. During locomotion, we were able to continuously monitor the stomach using the on-board camera (see Fig. 4).

V. Microgripper Deployment

A. Delivery Unit Actuation

The delivery unit of the MASCE consists of a magnetically activated fluid chamber that carries a large number of μ-grippers. Fig. 5 summarizes the activation mechanism. At the initial stage [see Fig. 5(a)], the lid of the chamber is fixed closed due to the magnetic attraction between the upper internal magnet of the MASCE (volume = V_u, magnetization = M_u) and the small magnet inside the lid (volume = V_s, magnetization = M_s). We can express this condition as

$$M_s V_s \frac{dB_u}{da}\Big|^{a=d_1} > M_s V_s \frac{dB_l}{da}\Big|^{a=L-d_1} \quad (1)$$

where a is the axis in the capsule length (magnetization) direction, B_u and B_l are the magnetic field generated from the upper and the lower internal magnet, respectively. The solution of (1) is $d_1 < 0.5L$. The length of the capsule, L, is not constant and changes as a function of the external magnetic field because the MASCE is axially contracted by the external magnetic field. However, we did not take this effect into account in our modeling because ΔL is negligible when the lid separates from the chamber.

In order to open up the chamber [see Fig. 5(b)], we need the lid to be separated from the top and drawn to the lower internal magnet of the MASCE. To break the equilibrium of the initial stage, we require an applied external field which satisfies the following equation:

$$M_s V_s \frac{dB_u}{da}\Big|^{a=d_1} < M_s V_s \frac{dB_l}{da}\Big|^{a=L-d_1} + M_s V_s \frac{dB_{\text{ext}}}{da}\Big|^{a=L-d_1+d_x} \quad (2)$$

where B_{ext} is the magnetic field generated by the external permanent magnet.

B. Distribution Experiments

To evaluate the targeting precision of the proposed μ-gripper distribution, we first filled the delivery unit of the MASCE with μ-grippers and placed it in a water bath. Using an external magnet, we activated the delivery unit to open up the chamber lid. We waited until the released μ-grippers touched down to the bottom surface, and then, took image snapshots with a hand-held camera. We estimated the position of each distributed μ-gripper using image processing techniques. Fig. 6 shows the percentage of the number of distributed μ-grippers as a function of the distance from the center of the capsule. In average, about 40% of μ-grippers (23 out of 66) distributed within 10-mm range.

VI. Retrieval of Microgrippers

A. Wet-adhesive Micropost Arrays

For this biopsy strategy, we fabricated the μ-grippers from nonmagnetic materials so that they were not affected by the magnets inside the MASCE as well as the applied external magnetic field during the gripper distribution. Since we cannot use magnetic attraction as the retrieval method, we utilized adhesive forces to collect the distributed μ-grippers. We created a wet-adhesive patch as a retrieval unit, which consists of micropost arrays and viscous silicone oil [23]. We chose silicone oil due to two main reasons. First, it is hydrophobic and hence does not mix with water resulting in very minimal loss during the biopsy procedure. Second, it has very high viscosity and thus can trap the grippers due to viscous forces.

Polyurethane elastomer micropost arrays in the retrieval unit perform three important roles. First, they increase the contact area of silicone oil and hence induce a strong bonding force between the micropost arrays and the silicone-oil, which increases the stability of the oil layer. Second, they minimize the mechanical loss of the silicone oil. If we press the silicone oil layer without the presence of microposts, the silicone oil layer will be pushed in the radial direction and we lose significant amount of oil during the process. Finally, the flexibility of the elastomer micropost arrays passively maximizes the contact area between the silicone oil and the uneven tissue surfaces.

We fabricated the retrieval unit following the steps summarized in Fig. 7. First, we used a rapid prototyping machine (Invision HR 3-D printer) to fabricate master plastic micropost arrays. Using this master, we created the silicone rubber cast and cured at 25 °C for 24 h. We, then, molded the micropost arrays using a polyurethane elastomer (ST-1060, BJB Enterprise Inc., Tustin, CA, USA). After removing the bubbles in the mold using a vacuum chamber, we pressed the mold with a cover and cured it for 8 h at 25 °C. Finally, we dipped the micropost arrays into highly viscous silicone oil (Dow Corning, silicone oil 200, 10 000 cSt) to complete the fabrication. Table II shows the specifications of the microposts and silicone oil. Fig. 8 shows the optical images of the resulting retrieval unit.

B. Adhesion Modeling

When particles interact with the silicone oil of the retrieval unit, they are trapped due to viscous forces (see Fig. 9). When we pull the retrieval unit in the z-direction [Fig. 9(b)], we indirectly create viscous force at the side space (F_{side}) and the upper space (F_{top}) of the trapped grippers.

F_{side} is generated due to the shear viscous force between the side wall of the microposts and the trapped grippers; and given by

$$F_{\text{side}}(r_o, r_p, h, b, u) = 2\int_0^{pi/2} \frac{\mu u r_o h}{x_c \sqrt{1+\tan^2\theta} - r_o} d\theta \quad (3)$$

$$x_c = \frac{b\tan\theta - \sqrt{b^2\tan^2\theta - (\tan^2\theta + 1)\,(b^2 - r_p^2)}}{\tan^2\theta + 1} \quad (4)$$

where r_o and h are the radius and the height of the particles, respectively, r_p is the radius of the micropost, b is the center-to-center distance between the grippers and the micropost, μ is the dynamic viscosity of the silicone oil, and u is the retraction velocity of the wet-adhesive patch. x_c is the x-position of the intersection point between the vector OC and the micropost [see Fig. 9(a)]. F_{side} can be numerically calculated using (3) and (4).

The second viscous force F_{top} is the Stefan adhesion, which is generated between the top surface of the trapped particles and the inner ceiling of the patch. This adhesion is induced by the squeezing flow of viscous liquid between two parallel disks [23], [24] and given by

$$F_{\text{top}}(r_o, s) = \frac{3\pi\mu r_o^4 u}{2s^3} \quad (5)$$

where s is the distance between the μ-grippers and the inner ceiling of the wet-adhesive patch. F_{top} dramatically decreases as s increases. The total wet-adhesive force is the sum of F_{top} and F_{side}. However, it is actually governed by F_{top} because s is small ($<100\,\mu$m) when the capsule is pulled toward tissue. Note that, even though (5) assumes a single-particle collection, it can be applied to multiparticle collection by adjusting r_0 for a lump of particles sticking together.

C. Model Validation

To validate the analytical adhesion model in (5), we measured the maximum wet adhesion of the retrieval unit at different retraction speeds. We built a force-controlled adhesion measurement setup as shown in Fig. 10. First, we trapped the tip of a small weight between the silicone oil-coated micropost arrays. Then, we pulled the retrieval unit up in constant speed using a motorized motion setup (Maxon RE 032). Changing the pulling speed, we measured the maximum weight that the retrieval unit can lift.

The adhesion force is at its maximum when the gap, s (see Fig. 9) is at its minimum. Therefore, if the maximum adhesive force is higher than the weight, the weight lifts as soon as the retrieval unit is pulled up before the gap, s, changes. Fig. 11 shows the maximum wet adhesion at each pulling speed, u. The curve-fitted data is almost linear as expected in (5). We calculated the gap, s, between the micropost and the retrieval unit from the slope of the plot as 113 μm. The real gap could not be measured directly, but the fitted gap value is reasonable because a thin oil film is expected between the weight and the adhesive patch.

VII. Biopsy Experiments

We conducted *ex vivo* biopsy experiments using a fresh pig stomach (see the supplementary multimedia extension for the video of the entire process). Since we already showed the magnetic manipulation of the capsule and the tissue monitoring performance of the camera

unit in previous sections, we focused only on the two critical steps of the proposed biopsy strategy: distribution and retrieval of μ-grippers.

First, we placed the tissue in a water bath at approximately 38 °C and waited until the tissue piece reached its equilibrium temperature. We loaded μ-grippers into the chamber using a glass pipette and filled the chamber with chilled water to prevent premature closing of μ-grippers in the chamber. We, then, moved the water bath to the maneuvering post where we used a cylindrical permanent magnet (diameter 50 mm × length 80 mm) to control the biopsy-MASCE. We dropped the μ-gripper-loaded biopsy-MASCE onto the tissue surface, manipulated it toward the center of the stomach tissue and activated the delivery unit to release μ-grippers (see Fig. 12). We manipulated the external magnet by hand while observing the biopsy-MASCE. To maintain the temperature of the water bath, we kept the time away from the hotplate to minimum.

After the deployment of the cargo, the μ-grippers, we placed the water bath back onto the hot plate to keep the temperature around 38 °C and waited for 10 min for μ-grippers to close. Using an optical microscope, we confirmed that μ-grippers were closed and attached to the tissue (see Fig. 13).

Finally, we used another capsule with the retrieval unit to collect the deployed μ-grippers (see Fig. 14). We repeated the retrieval process several times because our control on the biopsy-MASCE's position is not precise due to 1) manual positioning of the external magnet and 2) the wrinkles on the slippery gastric tissue surface. These processes also proved that the developed wet-adhesive patch is reusable in the wet environment.

We repeated the experiments with fresh pig stomach tissues 11 times and deployed approximately 2300 μ-grippers. We collected approximately 70 μ-grippers with the retrieval unit, resulting in a 3% retrieval rate. We stained the tissue retrieved by the biopsy-MASCE and used an optical microscope to confirm the success of the biopsy (see Fig. 15). The size of the extracted tissue samples is about 200–300 μm. Because the provided biopsy samples are tiny, genetic analyses are better suited to minimally invasive biopsy tools such as μ-grippers than conventional histological analyses [11], [25]. To fix the collected tissue, we soaked the retrieval units together with the retrieved μ-grippers and tissue in 4% paraformaldehyde (Sigma-Aldrich, Saint Luis, MO, USA) for about 20 min. We, then, permeabilized the tissue using chilled methanol. After rinsing with 1X PBS solution, we stained the tissue with 4′,6-diamidoino-2-phenylindole (DAPI) (Sigma-Aldrich, St. Louis, MO, USA) and rinsed it with PBS. After staining, we imaged the tissue under bright field and UV light. Fig. 16 shows the DAPI stained, retrieved tissue pieces where the blue color represent the stained cell nuclei confirming that the μ-gripper-loaded MASCE successfully retrieved cells.

VIII. Discussion

As highlighted in the introduction, previous biopsy mechanisms using capsule endoscopy have three main issues: precise targeting, navigation to a targeted position, and extracting multiple tissue samples. In this study, we combined the advantages of the MASCE with those of thermally activated μ-grippers to solve the aforementioned issues. Due to its

magnetically actuated rolling locomotion, the MASCE can navigate and reach a specified target. In this study, we showed that by carrying large numbers of μ-grippers as its cargo, the biopsy-MASCE was able to perform untethered, minimally invasive biopsy on stomach tissue. We also showed that by using hundreds of μ-grippers, we can retrieve multiple tissue samples around the deployed point and hence relax the need for highly accurate targeting.

While we successfully implemented the proposed biopsy strategy in *ex vivo* experiments, the biopsy-MASCE requires several critical improvements toward clinical applications in the future. First, we need to develop a 3-D localization method for the biopsy-MASCE. Multiobjective magnetic tracking algorithm using Levenberg–Marquardt optimization method [26] could be an appropriate localization method for the biopsy MASCE. This is also important for retrieving the distributed μ-grippers. Currently, they had to be collected blindly because the on-board camera is located on the other end of the capsule. If the biopsy-MASCE is localized and we can estimate the region of the distributed μ-grippers, even though they are not seen via the on-board camera directly, they could be collected precisely by the retrieval unit of the biopsy-MASCE.

The second limitation is the low yield (3%) of μ-gripper retrieval. In contrast, when we maneuvered the MASCE by hand to retrieve the μ-grippers, we collected approximately 20% of them. The difference between the two yield rates can be explained by the stronger preloading force. To reach this yield, one can increase the size and hence the magnetic field strength of the external magnet and utilize a robotic manipulator to maneuver it. As an alternative or enhancing solution, one could also increase the wet-adhesive force of the retrieval unit by using various biologically inspired wet adhesives [27]–[30]. Another solution to increase the retrieval rate is to further optimize the design variables of the micropost arrays such as the material, the height, the radius, and the center-to-center distance of the microposts. Since this paper shows the feasibility of the wet-adhesive mechanism, the technical point of the wet-adhesion method will be refined in the future by optimizing these design variables.

With regards to patient safety, we believe that the remaining, uncollected μ-grippers do not pose a significant risk when the biopsy is limited to the luminal gastrointestinal tract because those μ-grippers that are not attached to the tissue will easily be flushed away by peristalsis. The ones that are attached to the tissue might stay longer in the body; however, they too will be eventually cleared since the gastrointestinal mucosa is renewed within days to weeks and the old mucosa will be shed together with any remaining μ-grippers.

Another limitation of the current design is that one needs to collect the retrieval unit in order to analyze the extracted tissue samples. A simple, practical solution is to separate the retrieval unit from the capsule by pulling a flexible thin tether from the mouth. Although this feature was not demonstrated in the *ex vivo* experiments, it is not technically challenging because the wet-adhesive patches are designed to be easily uncapped. Moreover, the tethers for retrieving the wet-adhesive patch could also be used as wires providing power to the camera module and getting the video-output signal to prevent over-extending the size of the capsule.

Even though it is not directly related to the biopsy mechanism, we found that the rolling-based surface locomotion induces contamination on the camera module during *ex vivo* experiments. Covering the camera module with a specially designed optical dome will help decreasing the contamination when the stomach is filled with water. We are planning to implement a self-cleaning optical dome as a future research goal to address such contamination issues which exists for any capsule endoscope system.

IX. Conclusion

In this paper, we presented a new minimally invasive biopsy method using μ-grippers deployed and retrieved by the MASCE. We verified the feasibility of the proposed biopsy method in *ex vivo* experiments where we safely delivered thermo-sensitive, self-folding μ-grippers to a targeted area via the MASCE. We also showed that it is possible to utilize wet-adhesive forces to retrieve the distributed μ-grippers and the tissue samples collected by them. Although additional developments are required for the biopsy-MASCE to be used in clinical applications, this study shows that combining the advanced navigation skills of untethered magnetic capsule endoscopes with highly parallel, autonomous tissue sampling feature of self-folding μ-grippers promises a new strategy for gastrointestinal capsule biopsy.

Supplementary Material

Refer to Web version on PubMed Central for supplementary material.

Acknowledgments

This work of David H. Gracias was supported by the National Institutes of Health Director's New Innovator Award Program under grant DP2-OD004346-01, and the work of Metin Sitti and Sehyuk Yim was supported by the National Institutes of Health under Grant R01-NR014083.

References

1. Fireman Glukhovsky ZA, Scapa E. Future of capsule endoscopy. Gastrointestinal Endoscopy Clinic. Jan; 2004 14(1):219–227.
2. Moglia A, Menciassi A, Dario P, Cuschieri A. Capsule endoscopy: Progress update and challenges ahead. Nature Rev Gastroenterol Hepatol. Jun.2009 6:353–361. [PubMed: 19434097]
3. Toennies JL, Tortora G, Simi M, Valdastri P, Webster RJ III. Swallowable medical devices for diagnosis and surgery: The state of the art. J Mech Eng Sci. Jun; 2010 224(7):1397–1414.
4. Carpi F, Kastelein N, Talcott M, Pappone C. Magnetically controllable gastrointestinal steering of video capsules. IEEE Trans Biomed Eng. Feb; 2011 58(2):231–234. [PubMed: 20952324]
5. Hong Y, Kim J, Kwon Y, Song S. Preliminary study of a twistable thread module on a capsule endoscope in a spiral motion. Int J Precision Eng Manuf. 2011; 12(3):461–468.
6. Swain P, Toor A, Volke F, Keller J, Gerber J, Rabinovitz E, Rothstein R. Remote magnetic manipulation of a wireless capsule endoscope in the esophagus and stomach of humans. Gastrointestinal Endoscopy. Jun; 2010 71(7):1290–1293. [PubMed: 20417507]
7. Keller, H.; Juloski, A.; Kawano, H.; Bechtold, M.; Kimura, A.; Takizawa, H.; Kuth, R. Method for navigation and control of a magnetically guided capsule endoscope in the human stomach. Proc. IEEE RAS /EMBS Int. Conf. Biomed. Robot. Biomechatronics; Jun. 2012; p. 859-865.
8. Mahoney, AW.; Wright, SE.; Abbott, JJ. Managing the attractive magnetic force between an untethered magnetically actuated tool and a rotating permanent magnet," in. Proc. IEEE Int. Conf. Robot. Automation; 2013. p. 5346-5351.

9. Petruska, AJ.; Abbott, JJ. An omnidirectional electromagnet for remote manipulation. Proc. IEEE Int. Conf. Robot. Autom; 2013. p. 814-819.
10. Kong, K.; Cha, J.; Jeon, D.; Cho, D. A rotational micro biopsy device for the capsule endoscope. Proc. IEEE /RSJ Intell. Robots Syst; 2005. p. 1839-1843.
11. Park S, Koo K, Bang S, Park J, Song S, Cho D. A novel microactuator for microbiopsy in capsular endoscopes. J Micromechanics Microeng. 2007; 18(2):250–260.
12. Crosby WH, Kugler HW. Intraluminal biopsy of the small intestine. Amer J Digestive Dis. 1957; 2(5):236–241.
13. Simi M, Gerboni G, Menciassi A, Valdastri P. Magnetic torsion spring mechanism for a wireless biopsy capsule. ASME J Med Devices. Sep; 2013 7(4):041009-1–041009-9.10.1115/1.4025185
14. Kong K, Yim S, Choi S, Jeon D. A robotic biopsy device for capsule endoscopy. ASME J of Med Device. Jul; 2012 6(3):031004-1–031004-9.
15. Yim S, Sitti M. Design and rolling locomotion of a magnetically actuated soft capsule endoscope. IEEE Trans Robot. Jan; 2012 28(1):183–194.
16. Yim S, Goyal K, Sitti M. Magnetically actuated soft capsule with multi-modal drug release function. IEEE /ASME Trans Mechatronics. Aug; 2013 18(4):1413–1418.
17. Yim S, Sitti M. Shape-programmable soft capsule robots for semi-implantable drug delivery. IEEE Trans Robot. Oct; 2012 28(5):1198–1202.
18. Yim S, Sitti M. 3-D localization method for a magnetically actuated soft capsule endoscope and its applications. IEEE Trans Robot. Oct; 2013 29(5):1139–1151.
19. Gultepe E, Randhawa JS, Kadam S, Yamanaka S, Selaru FM, Shin EJ, Kalloo AN, Gracias DH. Biopsy with thermally-responsive untethered microtools. Adv Mater. Jan; 2013 25(4):514–519. [PubMed: 23047708]
20. Pandey S, Gultepe E, Gracias DH. Origami inspired self-assembly of patterned and reconfigurable particles. J Vis Exp. 2013; 72:e50022, 10.10.3791/50022 [PubMed: 23407436]
21. Leong T, Randall C, Benson B, Bassik N, Stern G, Gracias H. Tetherless thermobiochemically actuated micro-grippers. Proc Nat Acad Sci. Jan; 2009 106(3):703–708. [PubMed: 19139411]
22. Gultepe E, Yamanaka S, Laflin KE, Kadam S, Shim YS, Olaru AV, Limketkai B, Khashab MA, Kalloo AN, Gracias DH, Selaru FM. Biologic tissue sampling with untethered micro-grippers. Gastroenterology. Apr; 2013 144(4):691–693. [PubMed: 23399954]
23. Cheung E, Sitti M. Enhancing adhesion of biologically inspired polymer microfibers with a viscous oil coating. J Adhesion. Feb; 2011 87(6):547–557.
24. Bird, RB.; Armstrong, RC.; Hassager, O. Fluid Mechanics. 1. Vol. 1. Hoboken, NJ, USA: Wiley; 1977. Dynamics of polymeric liquids.
25. Cho WK, Ankrum JA, Guo D, Chestere SA, Yanga SY, Kashyap A, Campbella GA, Wood RJ, Rijala RK, Karnike R, Langer R, Karpa JM. Microstructured barbs on the North American porcupine quill enable easy tissue penetration and difficult removal. Proc Nat Acad Sci. Dec; 2012 109(52):21289–21294. [PubMed: 23236138]
26. Yang W, Hu C, Li M, Meng MQH, Song S. A new tracking system for three magnetic objectives. IEEE Trans Mag. Dec; 2010 46(12):4023–4029.
27. Lee H, Lee BP, Messersmith PB. A reversible wet/dry adhesive inspired by mussels and geckos. Nature. Jul.2007 448:338–342. [PubMed: 17637666]
28. Glass P, Chung H, Washburn NR, Sitti M. Enhanced reversible adhesion of dopamine methacrylamide-coated elastomer microfibrillar structures under wet Conditions. Langmuir. Jun; 2009 25(12):6607–6612. [PubMed: 19456091]
29. Glass P, Chung H, Washburn NR, Sitti M. Enhanced wet adhesion and shear of elastomeric micro-fiber arrays with mushroom tip geometry and a photopolymerized p(DMA-co-MEA) tip coating. Langmuir. Sep; 2010 26(22):17357–17362. [PubMed: 20879746]
30. Lee H, Scherer NF, Messersmith PB. Single-molecule mechanics of mussel adhesion. Proc Nat Acad Sci. Aug; 2006 103(35):12999–13003. [PubMed: 16920796]

Biographies

Sehyuk Yim (S'09) received the B.Eng. degree in mechanical engineering, the B.Eng. degree in electronic engineering, in 2007, and the M.S. degree in mechanical engineering in 2009, all from Sogang University, Seoul, Korea, and Ph.D. degree in mechanical engineering from Carnegie Mellon University, Pittsburgh, PA, USA, in 2012.

He is a postdoctoral research fellow in the Department of Mechanical Engineering, Carnegie Mellon University, since 2013. His current research interests include the design, modeling, and control of bioinspired robots, soft material robots for medical applications, modular robots, and programmable matter.

Evin Gultepe received the undergraduate degree and M.S. degrees with a thesis on statistical analysis of genetic information coding from Bogazici University, Istanbul, Turkey, and the Ph.D. from Department of Physics, Northeastern University, Boston, MA, USA, with a dissertation on applications of nanoplatforms in nanomanufacturing and nanomedicine.

She is a Postdoctoral Fellow at Johns Hopkins University, Baltimore, MD, USA, developing micro-surgical tools for minimally invasive medical procedures. She has coauthored 20 publications.

David H. Gracias (M'05) received the undergraduate degree from the Indian Institute of Technology, Kharagpur, India, and the Ph.D. from University of California, Berkeley, Berkeley, CA, USA, in 1999.

He is currently a Professor and Russell Croft Faculty Scholar in the Department of Chemical and Biomolecular Engineering, Johns Hopkins University (JHU), Baltimore, MD, USA. He did postdoctoral research at Harvard University and was a Senior Engineer at Intel Corporation prior to starting his independent career at JHU. His research interests include micro and nanotechnology and self-assembly. He has coauthored 92 journal publications, holds 22 patents.

Dr. Gracias received a number of awards including the NIH Director's New Innovator Award, NSF Career Award, Beckman Young Investigator Award, Camille Dreyfus Teaching Scholar Award, SPIE Nanoengineering Pioneer Award, and DuPont Young Professor Award.

Metin Sitti (S'94–M'00–SM'08) received the B.Sc. and M.Sc. degrees in electrical and electronics engineering from Bogazici University, Istanbul, Turkey, in 1992 and 1994, respectively, and the Ph.D. degree in electrical engineering from the University of Tokyo, Tokyo, Japan, in 1999.

He was a Research Scientist with the University of California at Berkeley during 1999–2002. He is currently a Professor with the Department of Mechanical Engineering and Robotics Institute, Carnegie Mellon University, Pittsburgh, PA, USA. He is the Director of the NanoRobotics Lab and Center for Bio-Robotics. His research interests include micro/nano-robotics, bioinspired, and biohybrid miniature mobile robots, bioinspired micro/nano-materials, and micro/nano-manipulation.

Dr. Sitti received the SPIE Nanoengineering Pioneer Award in 2011, National Science Foundation CAREER Award in 2005, and IBM Smarter Planet Award in 2012. He received the Best Paper Award in the IEEE/RSJ International Conference on Intelligent Robots and Systems in 2009 and 1998, the Best Biomimetics Paper Award at the IEEE Robotics and Biomimetics Conference in 2004, and the Best Video Award at the IEEE Robotics and Automation Conference in 2002. He was appointed as the Adamson Career Faculty Fellow during 2007–2010. He was the Vice President for Technical Activities at the IEEE Nanotechnology Council during 2008–2010. He was elected as the Distinguished Lecturer of the IEEE Robotics and Automation Society for 2006–2008. He is the current active Editor-In-Chief of *Journal of Micro-Bio Robotics*.

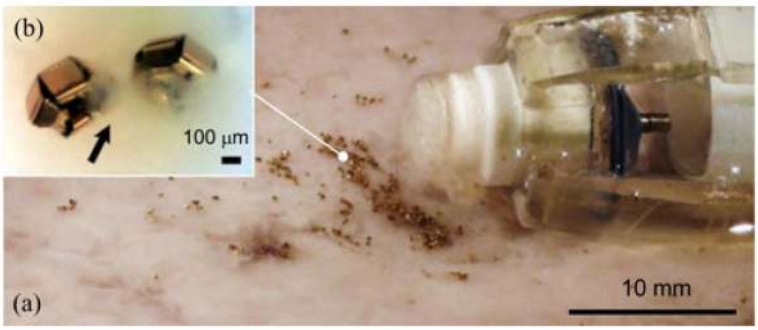

Fig. 1.

Biopsy using a *hierarchical microrobot*: (a) magnetically actuated capsule robot next to (b) the distributed self-folding μ-grippers. The developed magnetic capsule robot carries and releases untethered μ-grippers, and retrieves the tissue samples collected by μ-grippers. The arrow points out semitransparent tissue.

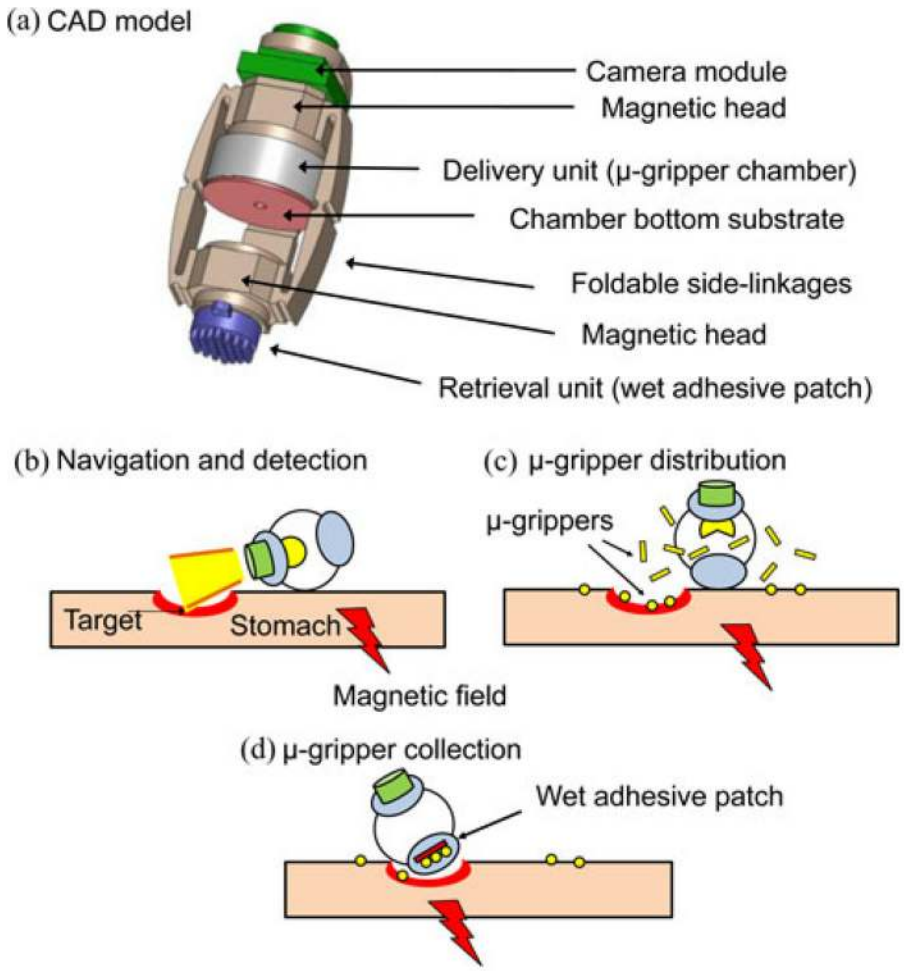

Fig. 2.

Schematic representation of a MASCE prototype with the proposed biopsy function. (a) CAD model of the MASCE. (b) Approaching the target by utilizing the external magnetic field. (c) Activating the delivery unit by the applied magnetic field and distributing the μ-grippers. (d) Collecting the μ-grippers and tissue samples via the retrieval unit (wet-adhesive patch).

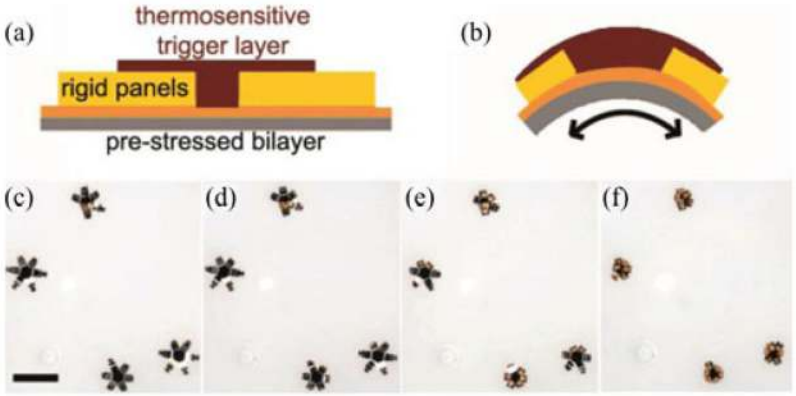

Fig. 3.

Thermo-sensitive, self-folding μ-grippers: Schematic of the pre-stressed hinges of μ-grippers in their (a) open and (b) closed states. (c)–(f) Bright field microscopy sequence showing μ-grippers closing in response to the temperature, 37 °C. Scale bar represents 1 mm.

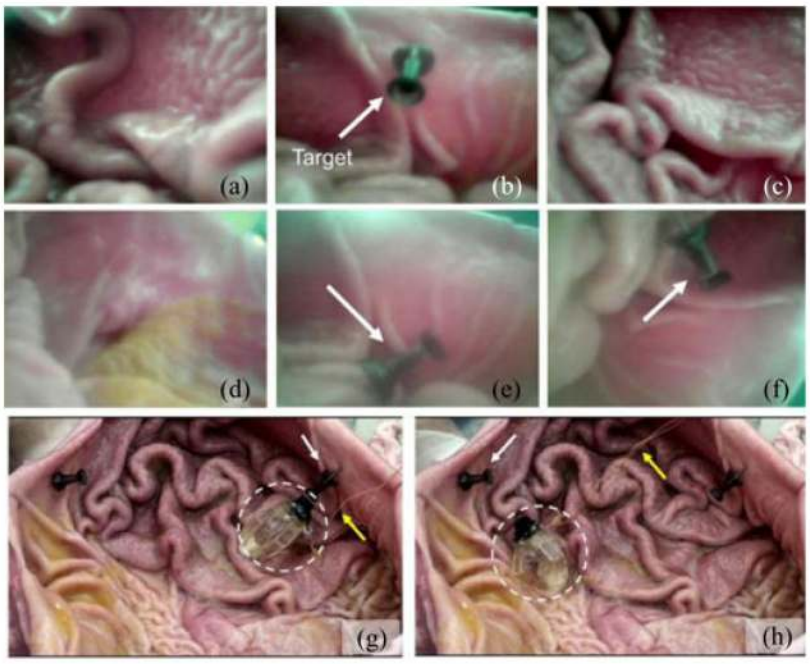

Fig. 4.

Images of the MASCE prototype approaching multiple targets inside a fresh pig stomach using its magnetically actuated rolling locomotion. (a)–(f) Images captured by the MASCE's on-board camera during navigation. (g)–(h) Snapshots of the MASCE in between targets. The targeted black pins are shown by the white arrows. The wires connected to the optical module are shown by the yellow arrows.

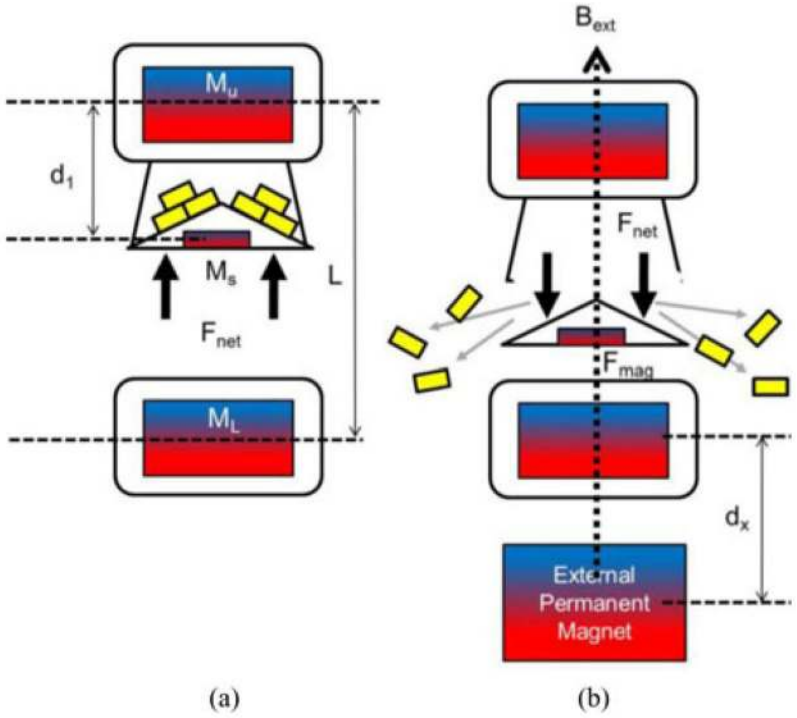

Fig. 5.

Schematics of the activation principle of the delivery unit. (a) The initial stage: the cargo chamber is anchored by the magnetic attraction between the upper magnet (M_u) and the small magnet (M_s) inside the lid. (b) The activated stage: The lid is separated from the chamber due to the external magnetic field and anchored to the lower magnet (M_l).

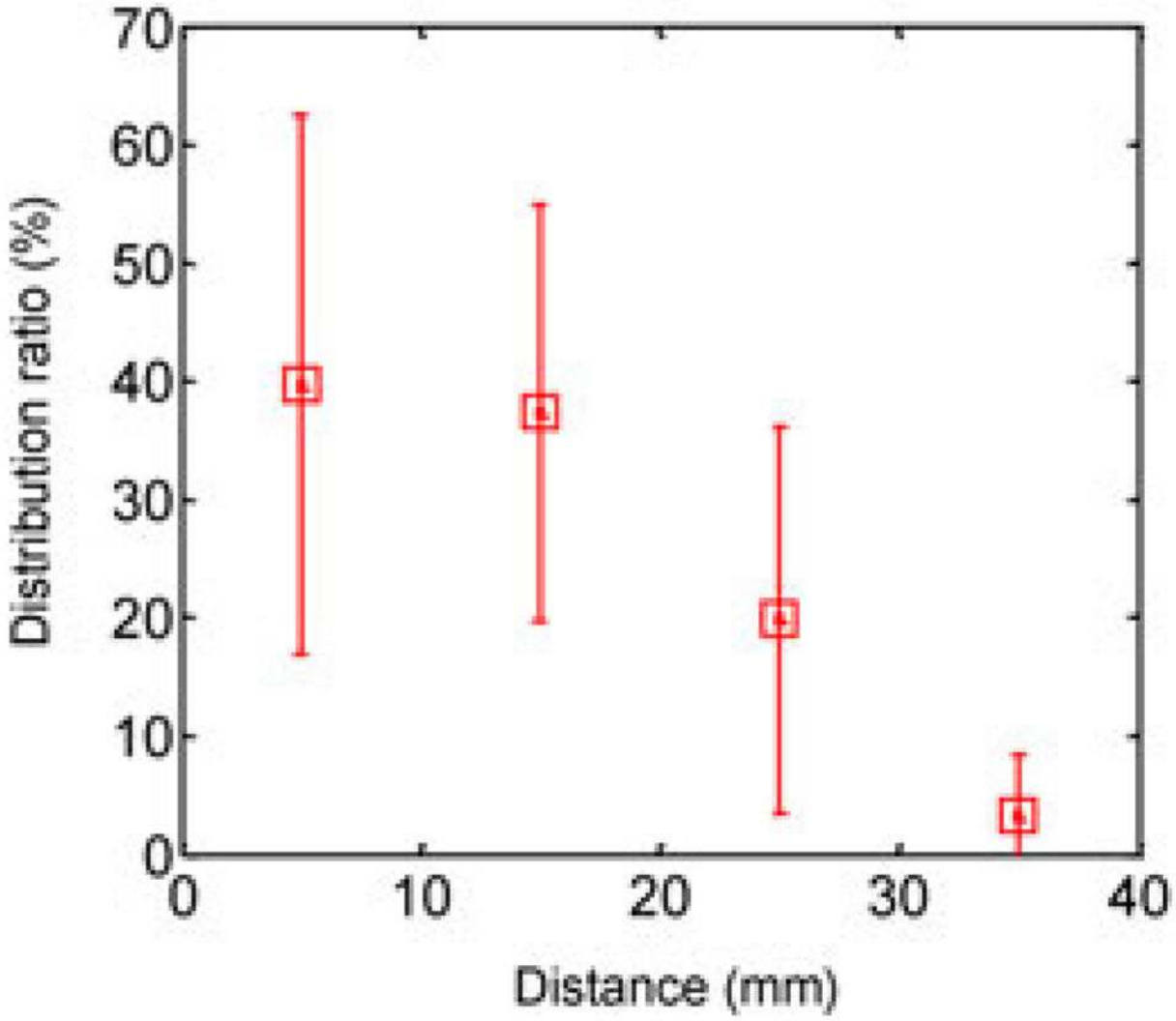

Fig. 6.

Distribution ratio of the μ-grippers as a function of the distance from the target. The total number of distributed μ-grippers was 66.

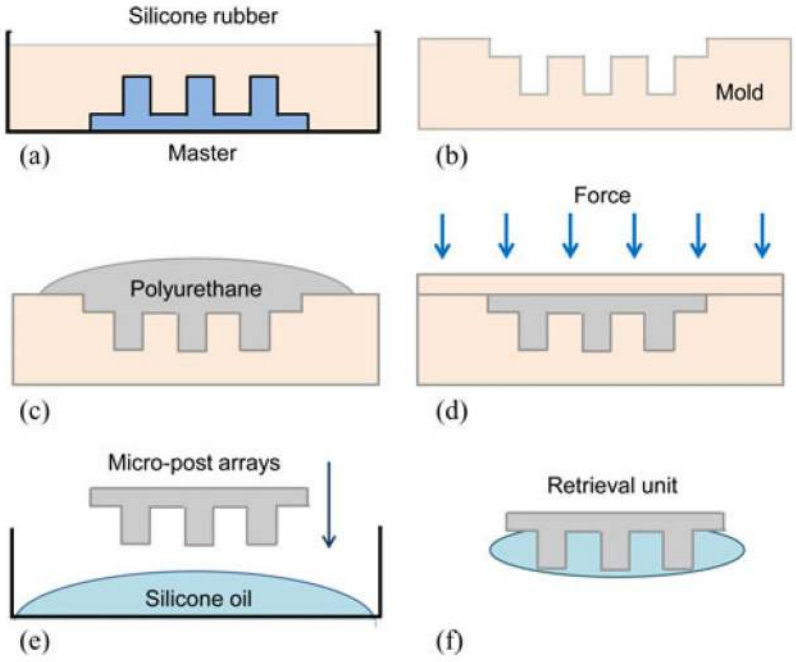

Fig. 7.

Schematics of the fabrication process of the μ-gripper retrieval components: (a) Molding and (b) curing the silicone rubber cast using a 3-D printed master, (c) molding and (d) curing of the elastomer micropost arrays, (e) covering the polyurethane micropost arrays with silicone oil, and (f) the resulting retrieval unit with silicone oil coated micropost arrays.

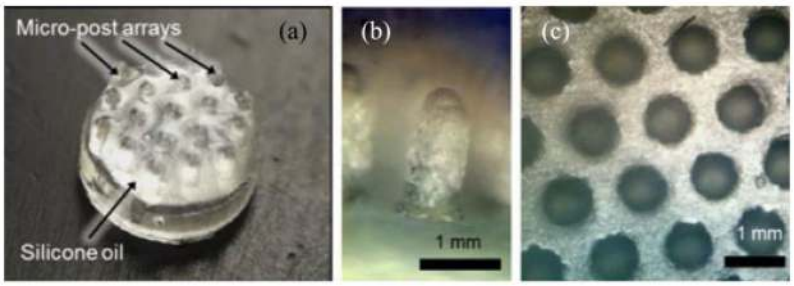

Fig. 8.

Bright-field optical microscopy images of the retrieval unit. (a) Wet-adhesive patch: silicone oil coated micropost arrays. (b) The side and (c) the top-view of the micropost arrays before coating with silicone oil. The microposts are arranged in a hexagonal lattice structure.

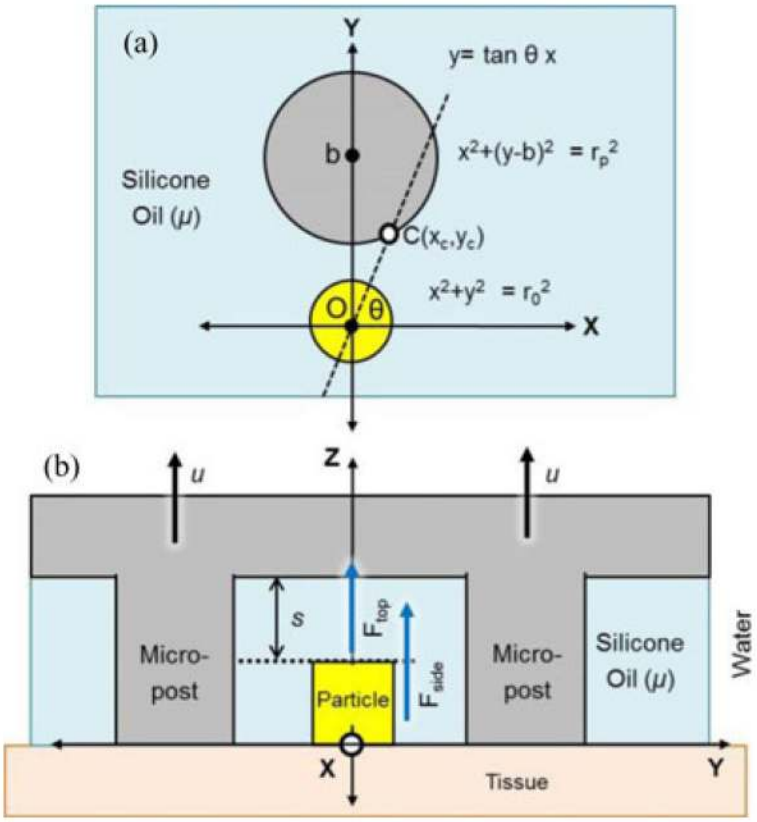

Fig. 9.

Schematic representations of the viscous forces between the retrieval unit and a trapped particle/μ-gripper: (a) top-view and (b) side-view.

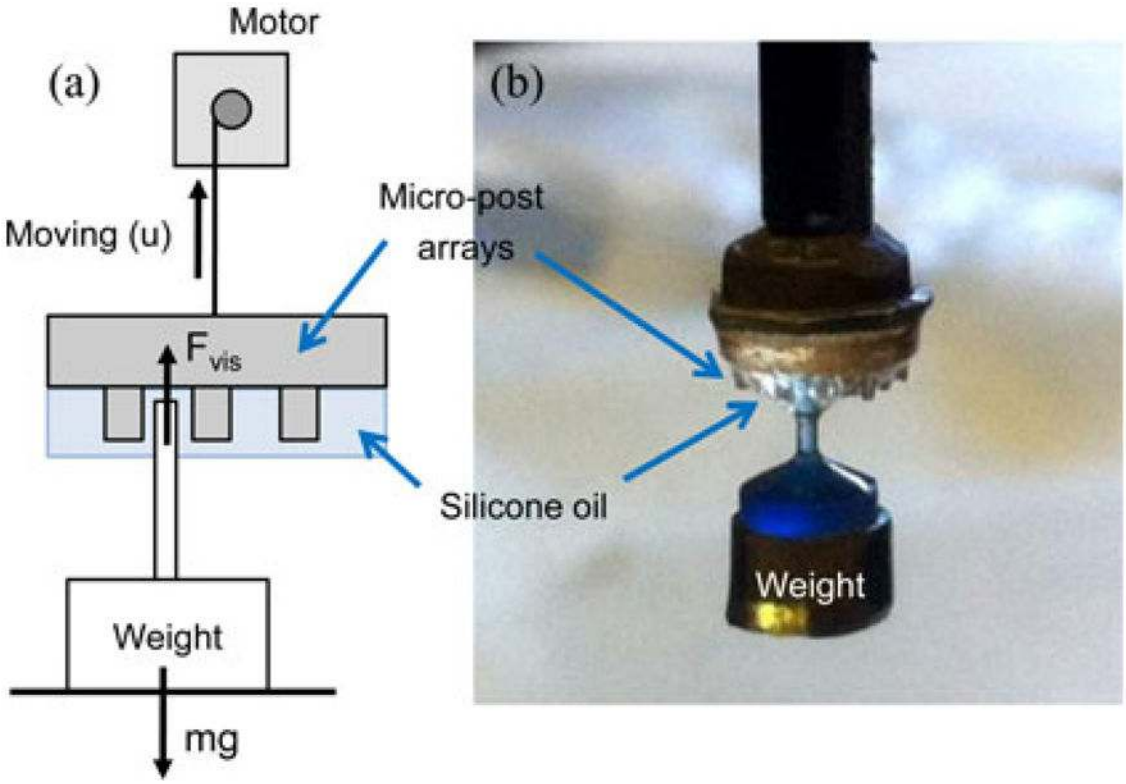

Fig. 10.

Wet-adhesive force measurement: (a) Schematic of the experimental setup. (b) Side-view photo of a weight lifted by the wet-adhesive patch pulled by the motorized setup.

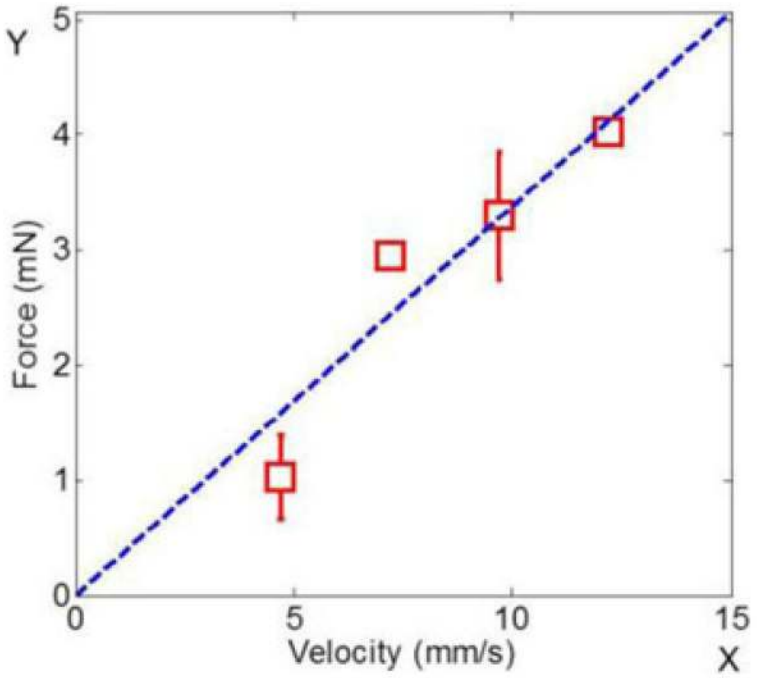

Fig. 11.

Maximum adhesive force of the retrieval unit as a function of pulling speed. The blue-dotted line is the fitted curve using the proposed model where $y = 0.338x$.

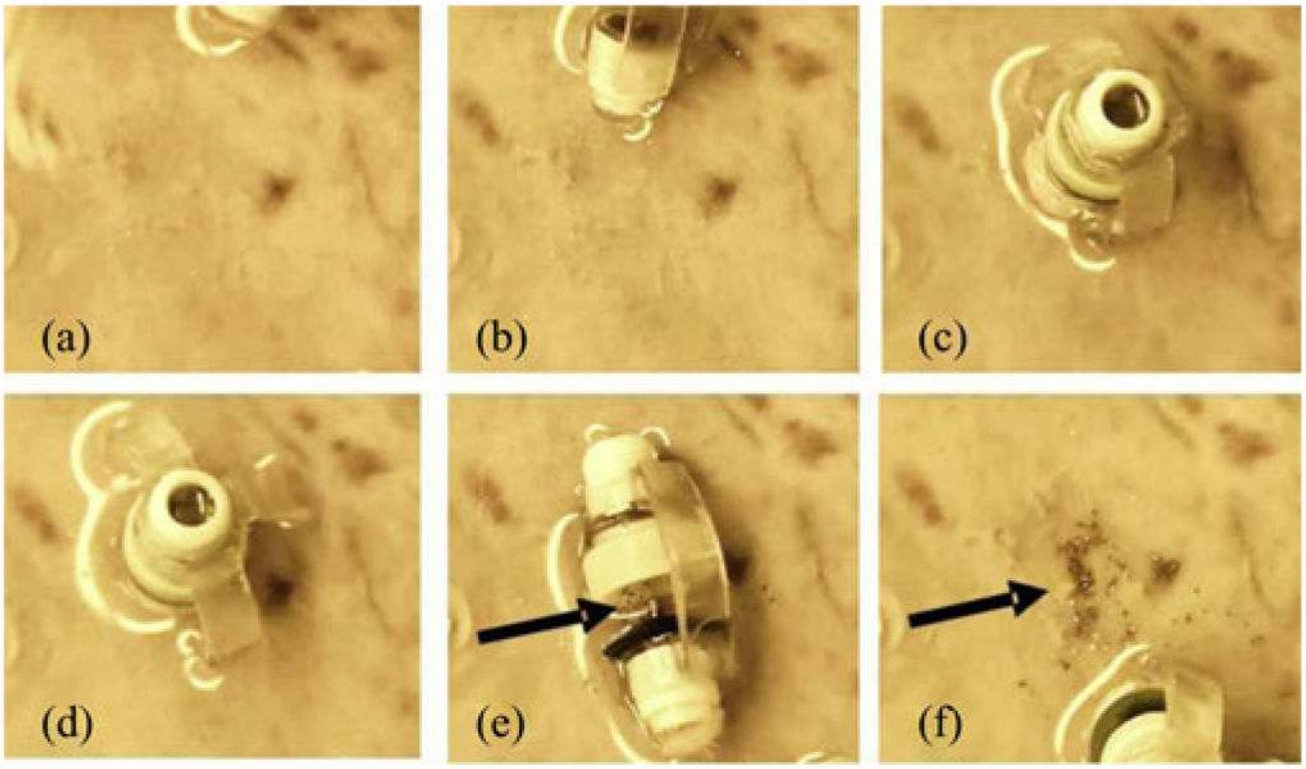

Fig. 12.

Snapshots of the magnetically controlled MASCE deploying its cargo, the μ-grippers, onto a fresh pig stomach tissue. Arrows point out the distributed μ-grippers.

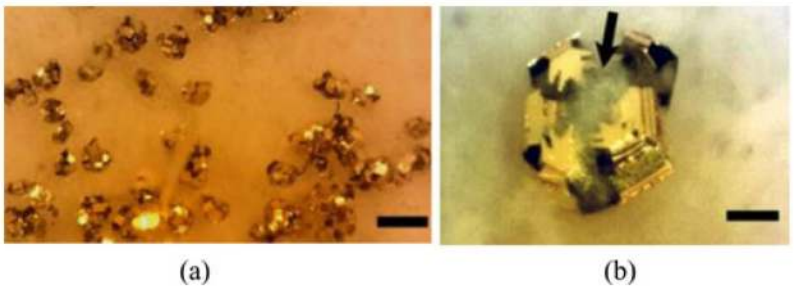

Fig. 13.

Bright-field optical microscopy images of deployed μ-grippers on a fresh pig stomach tissue. (a) 10 min after the deployment. The scale bar = 1 mm. (b) Close-up image showing a μ-gripper latching onto a piece of tissue. Arrow points out semitransparent tissue and the scale bar represent 100 μm.

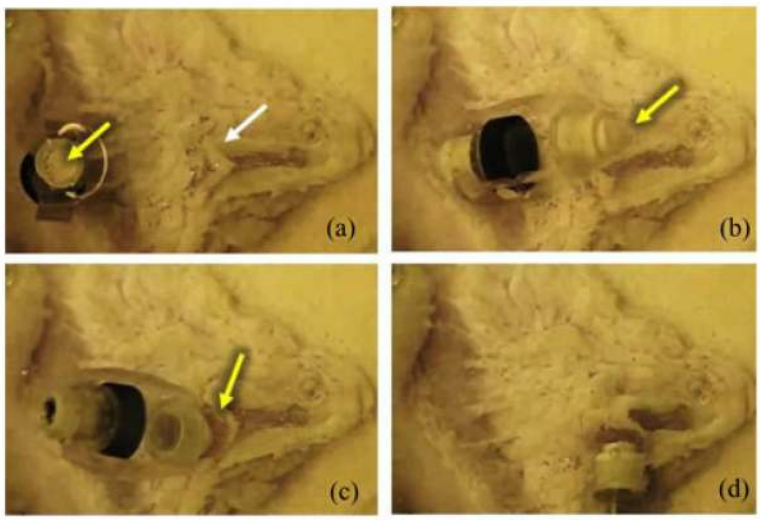

Fig. 14.

Snapshots of the magnetically controlled biopsy-MASCE retrieving the μ-grippers from the pig stomach tissue. The white arrow and the yellow arrows show the distributed μ-grippers and the wet-adhesive patch, respectively.

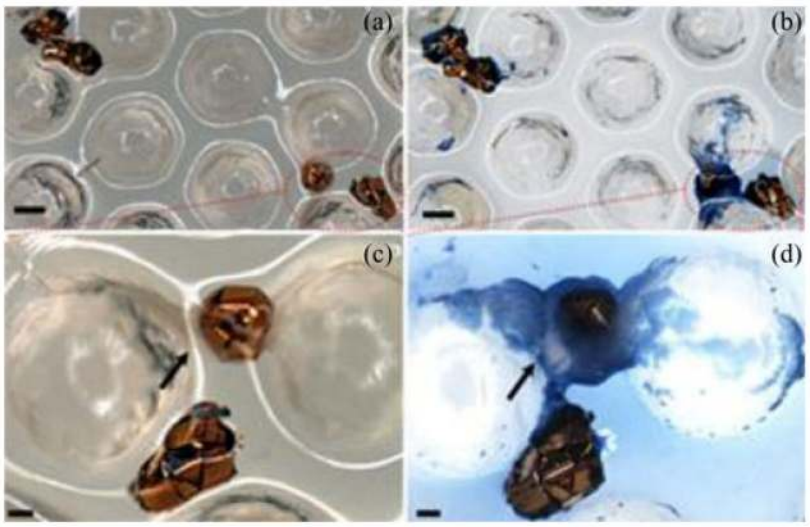

Fig. 15.

Optical microscope images of the retrieved μ-grippers: Bright field images of the retrieved μ-grippers (a) before and (b) after Trypan blue staining. The scale bars represent 300 μm. (c) and (d) Close-up bright field images showing μ-grippers latching onto tissue pieces: (c) before and (d) after Trypan blue staining. Arrows points out the collected tissue and the scale bars represent 100 μm.

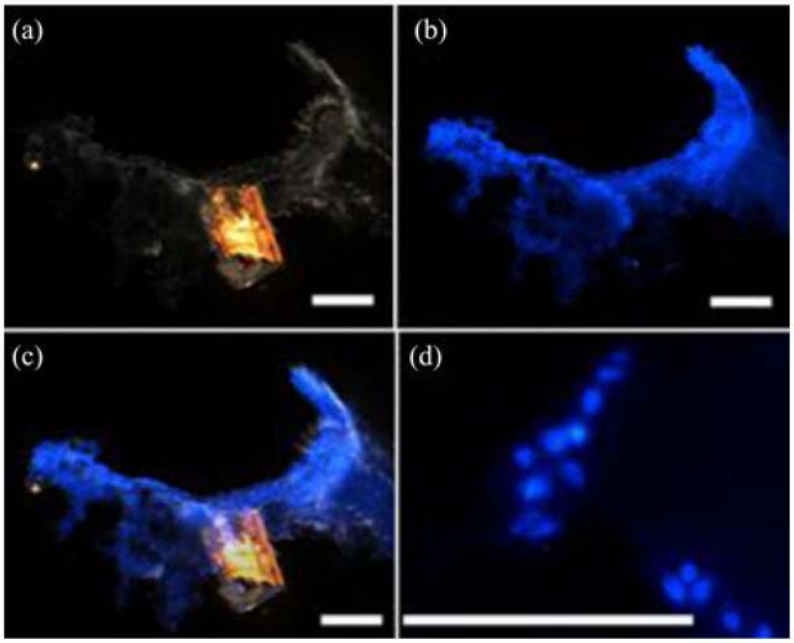

Fig. 16.

Optical images of the tissue retrieved by the μ-gripper loaded biopsy-MASCE and stained with DAPI: (a) Bright field, (b) fluorescence, and (c) overlay images. (d) High-resolution image of a tissue sample obtained with the μ-grippers showing individual DAPI-stained cell nuclei. Scale bars represent 100 μm.

TABLE I

Specifications of the Biopsy-MASCE Prototype

Size	
Normal state	
- Diameter (mm)	18
- Length (mm)	31.5*
Compressed state	
- Diameter (mm)	30
- Length (mm)	24*
Internal magnets	
Shape / Material	Cylindrical / NdFeB (N52)
Diameter / Thickness (mm)	6.4 / 6.4
Surface field (T)	0.523

* +8.7 mm with the camera.

TABLE II

Specifications of the Wet-Adhesive Patch

Micro-post	
Material	Polyurethane:(ST-1060, BJB Enterprise)
Tip diameter / Height (mm)	0.8 mm/ 1.5
Center distance (mm)	1.2
Number of posts	36
Silicone oil	
Viscosity (cSt)	10000
Density (g/cm^3)	0.971